

# Systematic and Dramatic Tuning on Gas Sorption Performance in Heterometallic Metal–Organic Frameworks

Quan-Guo Zhai,<sup>†</sup> Xianhui Bu,<sup>\*,‡</sup> Chengyu Mao,<sup>†</sup> Xiang Zhao,<sup>†</sup> and Pingyun Feng<sup>\*,†</sup>

<sup>†</sup>Department of Chemistry, University of California, Riverside, California 92521, United States

<sup>‡</sup>Department of Chemistry and Biochemistry, California State University, Long Beach, California 90840, United States

**S** Supporting Information

**ABSTRACT:** Despite their having much greater potential for compositional and structural diversity, heterometallic metal–organic frameworks (MOFs) reported so far have lagged far behind their homometallic counterparts in terms of CO<sub>2</sub> uptake performance. Now the power of heterometallic MOFs is in full display, as shown by a series of new materials (denoted CPM-200s) with superior CO<sub>2</sub> uptake capacity (up to 207.6 cm<sup>3</sup>/g at 273 K and 1 bar), close to the all-time record set by MOF-74-Mg. The isosteric heat of adsorption can also be tuned from −16.4 kJ/mol for CPM-200-Sc/Mg to −79.6 kJ/mol for CPM-200-V/Mg. The latter value is the highest reported for MOFs with Lewis acid sites. Some members of the CPM-200s family consist of combinations of metal ions (e.g., Mg/Ga, Mg/Fe, Mg/V, Mg/Sc) that have never been shown to coexist in any known crystalline porous materials. Such previously unseen combinations become reality through a cooperative crystallization process, which leads to the most intimate form of integration between even highly dissimilar metals, such as Mg<sup>2+</sup> and V<sup>3+</sup>. The synergistic effects of heterometals bestow CPM-200s with the highest CO<sub>2</sub> uptake capacity among known heterometallic MOFs and place them in striking distance of the all-time CO<sub>2</sub> uptake record.

Metal–organic framework (MOF) materials<sup>1,2</sup> are predominantly based on transition metals, and there are comparatively much fewer MOFs based on main-group elements. Despite such great disparity statistically favoring transition-metal MOFs, it is the magnesium form of MOF-74 (MOF-74-Mg) that exhibits the highest CO<sub>2</sub> uptake capacity (228 cm<sup>3</sup>/g at 273 K, 180 cm<sup>3</sup>/g at 298 K and 1 atm),<sup>3</sup> outshining its transition metal analogues such as MOF-74-Co and MOF-74-Ni and highlighting the unique significance of main-group metals in the design of high-performance gas sorption materials.

Advances with Mg-MOFs, in terms of gas sorption performance, stalled following the original discovery of MOF-74-Mg in 2008,<sup>3a</sup> as further exploration has yielded no new Mg-MOFs with CO<sub>2</sub> uptake capacity anywhere near that of MOF-74-Mg, casting doubts over the important role of main-group elements (Mg in particular) in MOF design. Given literature data illustrating respective advantages and disadvantages of different metals, we envisage a new family of high-performance materials that might be developed by some form of integration between different metals. This concept of heterometallic MOFs is by no means new, and the

challenge is how to deal with the infinite possibilities, and more so the perceived impossibilities, of combining metals to create high-performance materials. Prior to this work, there were few, if any, high-performance CO<sub>2</sub> capture materials based on heterometallic MOFs.

We are particularly interested in the integration of chemically dissimilar metals, as such combinations are more likely to lead to much greater variations in properties. Heterometallic MOFs containing similar metals (e.g., many combinations of 3d metals, any combination of 4f metals) are not uncommon. In addition, a number of heterometallic MOFs containing dissimilar metals (e.g., In and Co) have also been reported.<sup>4</sup> In general, dissimilar metals play distinct structural roles, as determined by their differing coordination properties such as radii, coordination geometry, and preference for donor atoms according to chemical hardness or softness. In most cases, dissimilar heterometals are separated by organic ligands, making them behave structurally in much the same way as in homometallic MOFs.<sup>5</sup>

Synergy between heterometals would most likely occur through the most intimate form of integration. In this work, we focus on a special family of heterometallic MOFs that are more difficult to prepare because they consist of dissimilar metal ions (e.g., Mg<sup>2+</sup> and V<sup>3+</sup>, or Ni<sup>2+</sup> and In<sup>3+</sup>) occupying crystallographically equivalent sites and exhibiting indistinguishable structural roles. Such an intimate form of integration between dissimilar metals allows both fine and dramatic tuning of their properties across a large range and all within the same framework type, which provides an unprecedented opportunity to probe the role of each metal type in the performance of new materials. For example, in this work, thanks to the diverse metal combinations in the same MOF framework, we demonstrate for the first time the observation of a strong correlation between isosteric heat for CO<sub>2</sub> and the charge-to-radius ratio ( $z/r$ ) of metal ions in MOFs.

It is not easy to integrate dissimilar metals in the same structural units. In fact, prior to this work, some metal combinations (such as Ga/Mg, Fe/Mg, V/Mg, and Sc/Mg reported here) have never been observed in any crystalline porous material. In fact, a grand challenge in materials design is to bring together chemical elements previously unknown to coexist. This is particularly true for crystalline materials prepared from low-temperature processes such as solution-based crystal growth, in which there is a great tendency for macroscopic phase separation. Some metal combinations reported are so unusual and unprecedented that we, ourselves, considered them highly unlikely prior to this study.

Received: December 27, 2015

Published: February 19, 2016

The synergistic effect of heterometals extends beyond structural, physical, and chemical properties in crystals, and it turned out that there is an unusual synergistic effect at the very beginning when two metals are brought together. In fact, the synergy during crystallization of CPM-200 is so essential that corresponding homometallic MOFs could not be made under the same conditions in the absence of any one of two metal sources.

We have systematically explored various metal combinations by focusing on the role of main-group elements. In addition, to study the effects of two main-group elements on Mg in Mg–Ga and Mg–In MOFs, Mg from the s-block and In from the p-block are used as the main-group elements for integration with transition metals, resulting in six more combinations (Mg with Sc, V, and Fe; In with Mn, Co, and Ni). Our method is quite general and is certainly capable of overcoming chemical dissimilarity.

Here, eight combinations between trivalent metals ( $M^{3+} = \text{In}^{3+}$ ,  $\text{Ga}^{3+}$ ,  $\text{Fe}^{3+}$ ,  $\text{V}^{3+}$ ,  $\text{Sc}^{3+}$ ) and divalent metals ( $M^{2+} = \text{Mg}^{2+}$ ,  $\text{Mn}^{2+}$ ,  $\text{Co}^{2+}$ ,  $\text{Ni}^{2+}$ ) were achieved for trimeric  $[\text{M}^{\text{II}}_2\text{M}^{\text{III}}(\mu_3\text{-OH})(\text{CO}_2)_6]$  clusters (Figure 1), leading to a series of MOFs (denoted here as

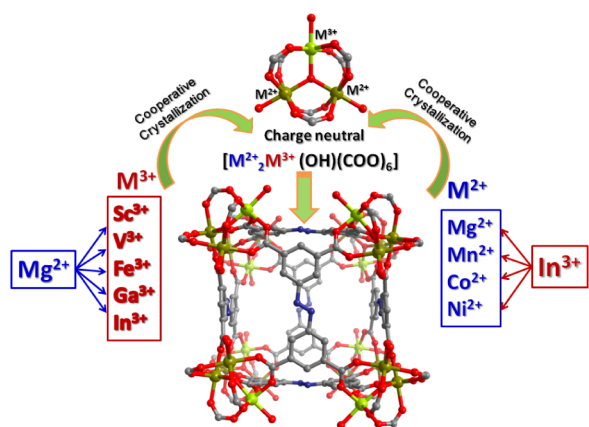


Figure 1.  $M^{2+}$  and  $M^{3+}$  combinations for CPM-200s in this work.

CPM-200-In/Mg, -In/Ni, -In/Co, -In/Mn, -Ga/Mg, -Fe/Mg, -V/Mg, and -Sc/Mg, where CPM = crystalline porous materials). Impressively, the  $\text{CO}_2$  uptakes of CPM-200-Fe/Mg and CPM-200-In/Mg at 273 K and 1 bar reach  $207.6 \text{ cm}^3 \text{ g}^{-1}$  ( $9.27 \text{ mmol/g}$ ) and  $190.8 \text{ cm}^3 \text{ g}^{-1}$  ( $8.52 \text{ mmol/g}$ ), which surpass the values of all reported MOFs based on  $[\text{M}_3(\mu_3\text{-O}/\text{OH})(\text{CO}_2)_6]$  and are also the highest among heterometallic MOFs. CPM-200-Fe/Mg is among the top four highest  $\text{CO}_2$  uptake MOFs under the same conditions. For MOFs made with ligands with  $-4$  (or less negative), CPM-200-Fe/Mg is only behind MOF-74-Mg.

A systematic search for a suitable cooperative crystallization condition is crucially important for the development of CPM-200s. For chemically dissimilar metals such as  $\text{Mg}^{2+}$  and  $\text{V}^{3+}$ , the rates of hydrolysis and condensation (olation for M-OH-M formation or oxolation for M-O-M formation) of each metal ion can differ greatly, negating any chance of cocrystallization. To achieve the matching kinetics for chemically dissimilar metal ions, we focused on the types of metal precursors, as well as types of and ratios between solvents and cosolvents. In this work, we first chose  $\text{In}^{3+}$  and  $\text{Mg}^{2+}$  to search for conditions capable of inducing cocrystallization of heterometals, because of our prior experience with In-MOFs<sup>6</sup> and Mg-MOFs<sup>7</sup> and because some metals such as  $\text{V}^{3+}$  and  $\text{Ga}^{3+}$  are known to be difficult to crystallize into MOFs. Numerous experiments led to the finding that the combination of  $\text{InCl}_3$  and  $\text{Mg}(\text{OAc})_2$  in DMA/ $\text{H}_2\text{O}$  (mass ratio = 5/1) is optimal

for the formation of pure CPM-200-In/Mg single crystals (see Supporting Information). A different DMA/water ratio gives a mixture of unknown yellow powder and cubic crystals, while  $\text{In}(\text{NO}_3)_3$  or  $\text{Mg}(\text{NO}_3)_2$  also gives yellow powder. Despite the essential role of  $\text{InCl}_3$  for making CPM-200-In/Mg,  $\text{InCl}_3$  itself fails to give the homometallic analogue, CPM-200-In. The use of only  $\text{Mg}(\text{OAc})_2$  was equally fruitless. Extension of the  $\text{In}^{3+}/\text{Mg}^{2+}$  cooperative crystallization method allows other members of the CPM-200s family to be made. It is worth emphasizing that the crystallization of homonuclear MOFs with only one metal source ( $\text{Ga}^{3+}$ ,  $\text{Fe}^{3+}$ ,  $\text{V}^{3+}$ , and  $\text{Sc}^{3+}$ , or  $\text{Mn}^{2+}$ ,  $\text{Co}^{2+}$ , and  $\text{Ni}^{2+}$ ) under the same reaction conditions was unsuccessful. All these demonstrate the importance of the cooperative crystallization.

Crystal structures of CPM-200-In/Mg, -In/Ni, -In/Co, -In/Mn, -Ga/Mg, and -V/Mg were determined by single-crystal X-ray diffraction (Tables S1–S3). The phase purity of all bulk samples was confirmed by powder X-ray diffraction (PXRD) (Figure S3). Due to the large difference in X-ray scattering factors, the  $M^{2+}$ -to- $M^{3+}$  ratio (2:1) could be determined by site occupancy refinement and further supported by EDS analysis (Figures S5 and S6). CPM-200s exhibit the soc-type framework topology (Figure S1), originally reported for an In-MOF with a cationic framework.<sup>8</sup> Heterometallic CPM-200s have a neutral framework due to the mixed  $M^{2+}/M^{3+}$ . Formation of the charge-neutral framework by taking advantage of the heterometallic cooperative crystallization process is quite general and can be applied to other trimer-based homonuclear MOFs as well.

To probe the effect of metal types on gas sorption properties, all as-synthesized CPM-200 samples were activated by immersion in  $\text{CH}_3\text{OH}$  for 3 days, followed by evacuation at  $80^\circ\text{C}$  for 12 h. The high framework stability was evident, as shown by the TGA results (Figure S4) and PXRD patterns (Figure S3). The  $\text{N}_2$  sorption isotherms of activated CPM-200s at 77 K all exhibit typical type I behavior (Figures 2 and S7–S17). Their Langmuir and BET surface areas vary from 1216 to 2024 and 877 to  $1459 \text{ cm}^2/\text{g}$ , respectively. In comparison, CPM-200-In with the cationic framework has Langmuir and BET surface areas of 1244 and  $888 \text{ cm}^2/\text{g}$ , respectively.

At 273 K and 1 bar, the  $\text{CO}_2$  uptakes by CPM-200s, in  $\text{cm}^3 \text{ g}^{-1}$  ( $\text{mmol/g}$ ), are 207.6 (9.27) for the Fe/Mg form, 190.8 (8.52) for In/Mg, 155.4 (6.94) for V/Mg, 136.9 (6.11) for In/Co, 136.2 (6.08) for Ga/Mg, 126.5 (5.65) for In/Mn, 122.4 (5.46) for Sc/Mg, and 100.4 (4.48) for In/Ni (Figures S7–S17 and Table S4). All these  $\text{CO}_2$  uptake values are impressive (Table S5). Even considering all MOFs, only Mg-MOF-74 ( $10.2 \text{ mmol/g}$ ),<sup>2b</sup> Cu-TDPAT ( $10.1 \text{ mmol/g}$ ),<sup>9</sup> and Cu-TPBTM ( $9.7 \text{ mmol/g}$ )<sup>10</sup> have higher  $\text{CO}_2$  uptake performance than CPM-200-Fe/Mg under the same conditions.

At 298 K and 1 bar, the  $\text{CO}_2$  uptakes by CPM-200s, in  $\text{cm}^3 \text{ g}^{-1}$ , are 127.3 (Fe/Mg), 113.7 (In/Mg), 80.4 (V/Mg), 79.2 (Ga/Mg), 77.6 (In/Co), 72.7 (In/Mn), 61.5 (In/Ni), and 61.4 (Sc/Mg) (Figures S7–S17 and Table S4). At these conditions, the  $\text{CO}_2$  uptake value of CPM-200-Fe/Mg is comparable to those of CPM-33b (126.4),<sup>11</sup> PCN-88 (123.2),<sup>12</sup> and SIFSIX-2-Cu-i (121.2)<sup>13</sup> and much higher than those of some well-known MOFs, including HKUST-1 (108.9),<sup>14</sup> en-Mg<sub>2</sub>(dobpdc) (102.4),<sup>15</sup> MAF-66 (98.8),<sup>16</sup> and bio-MOF-11 (91.8).<sup>17</sup>

For comparison, the  $\text{CO}_2$  uptake of homometallic CPM-200-In was also studied. It absorbs  $109.6 \text{ cm}^3/\text{g}$  ( $4.9 \text{ mmol/g}$ ) at 273 K and  $61.7 \text{ cm}^3/\text{g}$  ( $2.8 \text{ mmol/g}$ ) at 298 K and 1 bar. Clearly, introduction of  $M^{2+}$  ( $\text{Mg}^{2+}$ ,  $\text{Mn}^{2+}$ ,  $\text{Co}^{2+}$ ,  $\text{Ni}^{2+}$ ) dramatically tunes the  $\text{CO}_2$  uptake performance. In particular, it was observed that there is an increase in  $\text{CO}_2$  uptake for CPM-200 with increasing

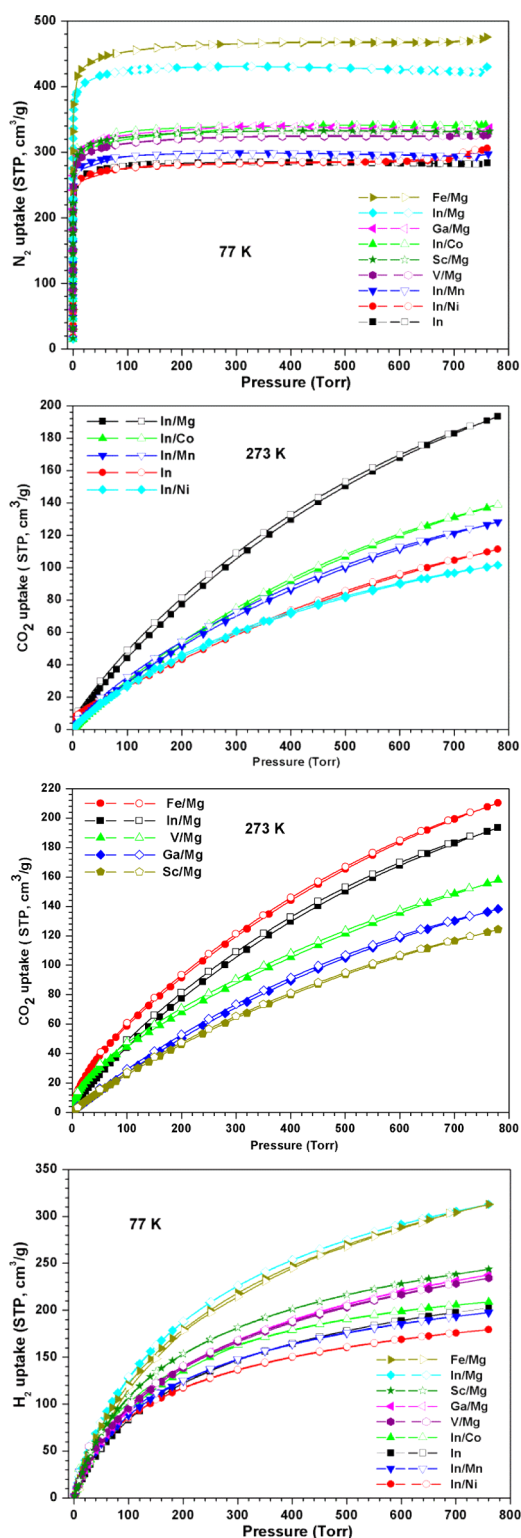


Figure 2.  $N_2$ ,  $CO_2$ , and  $H_2$  sorption study on CPM-200s.

Mg/In ratios (Figure S12), likely due to the increasing concentration of open  $Mg^{2+}$  sites. Changes in the framework charge and concentration of charge-balancing anions should also influence the gas uptake due to variations in electrostatic interactions and pore volume.

When  $In^{3+}$  was fixed, the  $CO_2$  uptakes of CPM-200-In/ $M^{II}$  followed the order  $Mg > Co > Mn > Ni$  (Figure 2), similar to that of MOF-74 with different metals.<sup>2a</sup> When  $Mg^{2+}$  was fixed,  $CO_2$

uptakes of CPM-200- $M^{III}$ /Mg followed the order  $Fe > In > V > Ga > Sc$  (Figure 2). In addition to the influence of molecular mass, the  $CO_2$  adsorption performance may be attributed to the interactions between  $CO_2$  and open metal sites.

To further understand  $CO_2$  adsorption properties of CPM-200s, the isosteric heat of adsorption ( $Q_{st}$ ) for  $CO_2$  was determined by fitting adsorption data collected at 273 and 298 K to the virial model (Figures S18–S20). At zero loading, indicative of the interaction of  $CO_2$  with open metal sites,  $Q_{st}^0$  (in kJ/mol) was determined to be  $-28.5$  (In/Ni),  $-25.0$  (In/Co),  $-27.3$  (In/Mn),  $-29.3$  (In/Mg),  $-19.7$  (Ga/Mg),  $-34.3$  (Fe/Mg),  $-79.6$  (V/Mg), and  $-16.4$  (Sc/Mg) (Figure 3).

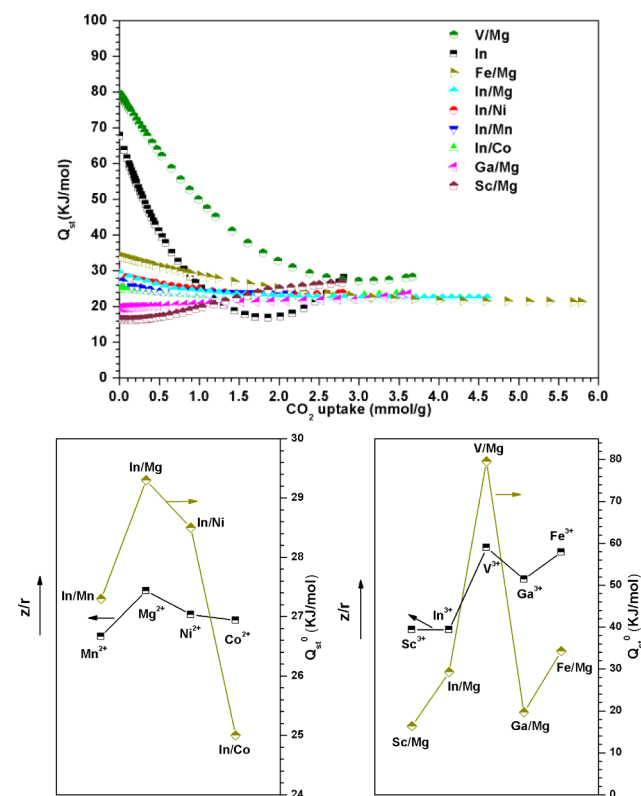


Figure 3. Top: Isosteric heat for  $CO_2$  for CPM-200s. Bottom: Correlation between isosteric heat at zero loading of  $CO_2$  ( $Q_{st}^0$ ) and charge-to-radius ratio ( $z/r$ ) of metal ions for CPM-200s.

Notably, the isosteric heat for CPM-200-V/Mg ( $-79.6$  kJ/mol) is higher than those of all reported MOFs containing open metal sites, and only lower than those of Cu-BTTri-mmen ( $-96$  kJ/mol)<sup>18</sup> and Cu-BTTri-en ( $-90$  kJ/mol)<sup>19</sup> with amines entrapped as Lewis base sites. This extremely high isosteric heat value is likely due to the additional contribution from vanadium ions, which may have significant  $\pi$  back-bonding. Based on such  $\pi$  back-bonding induced high interaction energies, hypothetical V-MOF-74 has been predicted to be the best MOF for  $N_2/CH_4$  separation.<sup>20</sup> Here, the  $V^{3+}/Mg^{2+}$  cooperative crystallization strategy may open up a new route for the development of V-MOFs. It is worth noting that CPM-200-In also exhibits a high  $Q_{st}^0$  for  $CO_2$  ( $-67.8$  kJ/mol), likely due to the charged framework.

The  $Q_{st}^0$  sequence matches well with the order of initial  $CO_2$  uptake values at very low pressure ( $<5$  Torr) (Figure S21), which indicates the contribution of open metal sites. To further understand the roles of metal ions, we examined their  $z/r$ ,

which is an important indication of electrostatic contribution to the bond energy and is related to the role of open metal sites on gas sorption properties. So far, no systematic correlation between  $z/r$  and  $Q_{st}^0$  has been observed for MOFs. Here, with the availability of a series of heterometallic MOFs, for the first time, we are able to clearly observe a strong correlation between  $z/r$  and the isosteric heat for  $CO_2$  (Figure 3).

The sorption properties of three fuel molecules (i.e.,  $H_2$ ,  $C_2H_2$ , and  $CH_4$ ) were also studied. At 77 K and 1 bar, CPM-200-Fe/Mg and -In/Mg both adsorb 2.8 wt%  $H_2$  (Figure 2), while values for other CPM-200s range from 1.6 to 2.2 wt%  $H_2$  (Table S4). At 1 bar, the uptake capacity of CPM-200-Fe/Mg for  $C_2H_2$  and  $CH_4$  reaches 217.2 and 39.5  $cm^3/g$ , respectively, at 273 K and 160.8 and 23.5  $cm^3/g$  at 298 K. Other CPM-200s also show superior sorption performance for  $C_2H_2$  at 273 K (Table S4).

CPM-200s show negligible  $N_2$  uptake performance at 273 K (Figure S22). To predict  $CO_2$ - $N_2$  binary mixture selectivity, an ideal adsorbed solution theory calculation based on a dual-site Langmuir–Freundlich simulation was employed, based on single-component  $CO_2$  and  $N_2$  adsorption isotherms. Figure S22 shows the adsorption selectivity of five members of CPM-200s for  $CO_2$  (50%) and  $N_2$  (50%) at 273 K. The selectivity values vary from 406 (V/Mg), 201 (Fe/Mg), 48 (In/Mg), 33 (In/Co), to 24 (Ga/Mg), which are higher than those of many other MOFs.<sup>1g,21</sup> Since the order matches well with the  $Q_{st}^0$  sequence, such tunable  $CO_2$  selectivity over  $N_2$  could be attributed to the different interactions between gas molecules and open metal sites.

In summary, a family of heterometallic MOFs (CPM-200 series) with systematic and unprecedented combinations of trivalent ( $In^{3+}$ ,  $Ga^{3+}$ ,  $Fe^{3+}$ ,  $V^{3+}$ ,  $Sc^{3+}$ ) and divalent metals ( $Mg^{2+}$ ,  $Mn^{2+}$ ,  $Co^{2+}$ ,  $Ni^{2+}$ ) has been achieved. Even metal ions difficult in MOF synthesis (e.g.,  $Ga^{3+}$ ,  $V^{3+}$ ) succumb to this cooperative crystallization strategy and become MOF-friendly. Significantly, CPM-200-Fe/Mg can adsorb  $CO_2$ , 9.27 mmol/g at 273 K and 1 bar, which outperforms all trimer-based as well as all heterometallic MOFs. It is among the top four highest  $CO_2$  uptake MOFs under the same conditions. The isosteric heat of adsorption for  $CO_2$  binding in CPM-200-V/Mg,  $-79.6$  kJ/mol, is the highest reported for MOFs with Lewis acid sites. Finally, with various combinations of metal ions in the same MOF platform, a strong correlation between charge-to-radius ratio of metal cations and isosteric heat for  $CO_2$  has been established for the first time in MOFs.

## ■ ASSOCIATED CONTENT

### 📄 Supporting Information

The Supporting Information is available free of charge on the ACS Publications website at DOI: 10.1021/jacs.5b13491.

Experimental details, Figures S1–S22, and Tables S1–S5 (PDF)

X-ray crystallographic data for six CPM-200s (CCDC 1444374–1444379) (CIF)

## ■ AUTHOR INFORMATION

### Corresponding Authors

\*xianhui.bu@csulb.edu

\*pingyun.feng@ucr.edu

### Notes

The authors declare no competing financial interest.

## ■ ACKNOWLEDGMENTS

The work is supported by the US Department of Energy, Office of Basic Energy Sciences, Materials Sciences and Engineering Division under award No. DE-FG02-13ER46972.

## ■ REFERENCES

- (a) Jiang, J.; Yaghi, O. M. *Chem. Rev.* **2015**, *115*, 6966. (b) O’Keeffe, M.; Yaghi, O. M. *Chem. Rev.* **2012**, *112*, 675. (c) Phan, A.; Doonan, C. J.; Uribe-Romo, F. J.; Knobler, C. B.; O’Keeffe, M.; Yaghi, O. M. *Acc. Chem. Res.* **2010**, *43*, 58. (d) Zhou, H.-C.; Long, J.; Yaghi, O. M. *Chem. Rev.* **2012**, *112*, 673. (e) Farha, O. K.; Hupp, J. T. *Acc. Chem. Res.* **2010**, *43*, 1166. (f) Tanabe, K. K.; Cohen, S. M. *Chem. Soc. Rev.* **2011**, *40*, 498. (g) Sumida, K.; Rogow, D. L.; Mason, J. A.; McDonald, T. M.; Bloch, E. D.; Herm, Z. R.; Bae, T.-H.; Long, J. R. *Chem. Rev.* **2012**, *112*, 724.
- (a) Yaghi, O. M.; O’Keeffe, M.; Ockwig, N. W.; Chae, H. K.; Eddaoudi, M.; Kim, J. *Nature* **2003**, *423*, 705. (b) Cho, H. S.; Deng, H.; Miyasaka, K.; Dong, Z.; Cho, M.; Neimark, A. V.; Kang, J. K.; Yaghi, O. M.; Terasaki, O. *Nature* **2015**, *527*, 503.
- (a) Caskey, S. R.; Wong-Foy, A. G.; Matzger, A. J. *J. Am. Chem. Soc.* **2008**, *130*, 10870. (b) Yang, D.; Cho, H.; Kim, J.; Yang, S.; Ahn, W. *Energy Environ. Sci.* **2012**, *5*, 6465.
- (a) Zheng, S.-T.; Wu, T.; Chou, C.; Fuhr, A.; Feng, P.; Bu, X. *J. Am. Chem. Soc.* **2012**, *134*, 4517. (b) Zheng, S.-T.; Zhao, X.; Lau, S.; Fuhr, A.; Feng, P.; Bu, X. *J. Am. Chem. Soc.* **2013**, *135*, 10270. (c) Zheng, S.-T.; Mao, C.; Wu, T.; Lee, S.; Feng, P.; Bu, X. *J. Am. Chem. Soc.* **2012**, *134*, 11936. (d) Sajna, K. V.; Fracaroli, A. M.; Yaghi, O. M.; Tashiro, K. *Inorg. Chem.* **2015**, *54*, 1197. (e) Wang, L. J.; Deng, H.; Furukawa, H.; Gándara, F.; Cordova, K. E.; Peri, D.; Yaghi, O. M. *Inorg. Chem.* **2014**, *53*, 5881.
- (a) Zhang, M. B.; Zhang, J.; Zheng, S. T.; Yang, G. Y. *Angew. Chem., Int. Ed.* **2005**, *44*, 1385. (b) Wang, X. Y.; Avendaño, C.; Dunbar, K. R. *Chem. Soc. Rev.* **2011**, *40*, 3213.
- (a) Zheng, S.-T.; Bu, J. T.; Li, Y.; Wu, T.; Zuo, F.; Feng, P.; Bu, X. *J. Am. Chem. Soc.* **2010**, *132*, 17062. (b) Zheng, S.-T.; Bu, J. J.; Wu, T.; Chou, C.; Feng, P.; Bu, X. *Angew. Chem., Int. Ed.* **2011**, *50*, 8858.
- Zhai, Q.-G.; Lin, Q.; Wu, T.; Zheng, S.-T.; Bu, X.; Feng, P. *Dalton Trans.* **2012**, *41*, 2866.
- Liu, Y.; Eubank, J. F.; Cairns, A. J.; Eckert, J.; Kravtsov, V. C.; Luebke, R.; Eddaoudi, M. *Angew. Chem., Int. Ed.* **2007**, *46*, 3278.
- Li, B.; Zhang, Z.; Li, Y.; Yao, K.; Zhu, Y.; Deng, Z.; Yang, F.; Zhou, X.; Li, G.; Wu, H.; Nijem, N.; Chabal, Y. J.; Lai, Z.; Han, Y.; Shi, Z.; Feng, S.; Li, J. *Angew. Chem., Int. Ed.* **2012**, *51*, 1412.
- Zheng, B.; Bai, J.; Duan, J.; Wojtas, L.; Zaworotko, M. J. *J. Am. Chem. Soc.* **2011**, *133*, 748.
- Zhao, X.; Bu, X.; Zhai, Q.; Tran, H.; Feng, P. *J. Am. Chem. Soc.* **2015**, *137*, 1396.
- Li, J. R.; Yu, J.; Lu, W.; Sun, L. B.; Sculley, J.; Balbuena, P. B.; Zhou, H. C. *Nat. Commun.* **2013**, *4*, 1538.
- Nugent, P.; Belmabkhout, Y.; Burd, S. D.; Cairns, A. J.; Luebke, R.; Forrest, K.; Pham, T.; Ma, S.; Space, B.; Wojtas, L.; Eddaoudi, M.; Zaworotko, M. J. *Nature* **2013**, *495*, 80.
- Wang, Q. M.; Shen, D.; Bülow, M.; Lau, M.; Deng, S.; Fitch, F. R.; Lemcoff, N. O.; Semanscin, J. *Microporous Mesoporous Mater.* **2002**, *55*, 217.
- Lee, W. R.; Hwang, S. Y.; Ryu, D. W.; Lim, K. S.; Han, S. S.; Moon, D.; Choi, J.; Hong, C. S. *Energy Environ. Sci.* **2014**, *7*, 744.
- Lin, R. B.; Chen, D.; Lin, Y. Y.; Zhang, J. P.; Chen, X. M. *Inorg. Chem.* **2012**, *51*, 9950.
- An, J.; Geib, S. J.; Rosi, N. L. *J. Am. Chem. Soc.* **2010**, *132*, 38.
- McDonald, T. M.; D’Alessandro, D. M.; Krishna, R.; Long, J. R. *Chem. Sci.* **2011**, *2*, 2022.
- Demessence, A.; D’Alessandro, D. M.; Foo, M. L.; Long, J. R. *J. Am. Chem. Soc.* **2009**, *131*, 8784.
- Lee, K.; Isley, W. C.; Dzubak, A. L.; Verma, P.; Stoneburner, S. J.; Lin, L.; Howe, J. D.; Bloch, E. D.; Reed, D. A.; Hudson, M. R.; Brown, C. M.; Long, J. R.; Neaton, J. B.; Smit, B.; Cramer, C. J.; Truhlar, D. G.; Gagliardi, L. *J. Am. Chem. Soc.* **2014**, *136*, 698.
- Xiong, S.; Gong, Y.; Wang, H.; Wang, H.; Liu, Q.; Gu, M.; Wang, X.; Chen, B.; Wang, Z. *Chem. Commun.* **2014**, *50*, 12101.